The effect of deformation dependent permittivity on the elastic response of a finitely deformed dielectric tube

** Dedicated to the memory of our distinguished colleague Gérard Maugin **

Luis Dorfmann

Department of Civil and Environmental Engineering,
Tufts University, Medford, MA 02155, USA

Ray W. Ogden

School of Mathematics and Statistics,
University of Glasgow, Glasgow G12 8SQ, UK

Abstract

In this paper the influence of a radial electric field generated by compliant electrodes on the curved surfaces of a tube of dielectric electroelastic material subject to radially symmetric finite deformations is analyzed within the framework of the general theory of nonlinear electroelasticity. The analysis is illustrated for two constitutive equations based on the neo-Hookean and Gent elasticity models supplemented by an electrostatic energy term with a deformation dependent permittivity.

Keywords: Nonlinear electroelasticity, deformation dependent permittivity, dielectric elastomer tube

1. Introduction

A recent paper by Melnikov and Ogden [1] was concerned with the analysis of the extension and inflation of a circular cylindrical tube of dielectric elastomer material subject to a radial electric field produced by a potential difference between compliant electrodes on its curved surfaces. The dielectric properties of the material were defined by a constant permittivity, and we refer to [1] for discussion of the relevant background references and motivation. In the present work we extend that analysis to take additional account of torsion applied to the tube and, importantly, to allow for the permittivity of the material to be deformation dependent, in recognition of experimental findings of such dependence (see, for example, [2, 3]). Aspects of the modelling of strain-dependent permittivity have been examined in [4, 5, 6], for example.

In Section 2 we summarize briefly the basic equations of the theory of nonlinear electroelasticity that are needed for the subsequent analysis. Then, in Section 3, the equations are specialized to the geometry of a circular cylindrical tube subject to extension, inflation and torsion in the presence of a radial electric field. Irrespective of the particular form of the electroelastic constitutive law for the material of the tube, general formulas are obtained for the internal pressure, reduced axial load and torsional moment. The more restricted problem of a circular cylindrical tube subject to an axial load and a radial electric field, without internal pressure or torsion, was discussed in [7].

The general results are applied in Section 4 to the neo-Hookean elastic model with an electrostatic energy depending on a deformation dependent permittivity. For this model analytical solutions are obtained for the pressure, reduced axial load and torsional moment in terms of the deformation and electric parameters. The results highlight, in particular, the strong influence of both the deformation dependent permittivity and the torsion in comparison with the results for zero torsion and constant permittivity obtained in [1].

The Gent model [8] provides an alternative form of the elastic part of the energy function and, by contrast with the neo-Hookean model, accounts for the rapidly stiffening response of the material at large deformations. For this reason, Section 5 provides details of results for the Gent model analogous to those in Section 4, the differences associated with the strain stiffening being highlighted. Section 6 contains a few closing remarks.

In paying tribute to the memory of Gérard Maugin, we would particularly like to acknowledge the influence of his works summarized in the volumes [9, 10].

2. Basic equations

2.1. Kinematics

Consider a material body in a stress-free undeformed configuration that is used as the *reference* configuration $\mathcal{B}_\mathrm{r}$ with boundary $\partial\mathcal{B}_\mathrm{r}$. Let a typical material point in this configuration be identified by its position vector $\mathbf{X}$. The configuration and boundary of the body, after deformation from $\mathcal{B}_\mathrm{r}$, are denoted $\mathcal{B}$ and $\partial\mathcal{B}$, respectively. The corresponding position vector is denoted $\mathbf{x}$ and the quasi-static deformation from $\mathcal{B}_\mathrm{r}$ to $\mathcal{B}$ is written $\mathbf{x} = \boldsymbol{\chi}(\mathbf{X})$, where the vector function $\boldsymbol{\chi}$ defines the deformation. It follows that the deformation gradient tensor $\mathbf{F}$ is given

by $\mathbf{F} = \mathrm{Grad}\boldsymbol{\chi}(\mathbf{X})$, where Grad is the gradient operator with respect to $\mathbf{X}$. For incompressible materials, to which attention is confined here, the constraint $\det\mathbf{F} = 1$ must be satisfied.

Associated with $\mathbf{F}$ are the right and left Cauchy–Green deformation tensors, denoted $\mathbf{C}$ and $\mathbf{B}$ respectively and defined by

$$\mathbf{C} = \mathbf{F}^{\mathrm{T}}\mathbf{F}, \quad \mathbf{B} = \mathbf{F}\mathbf{F}^{\mathrm{T}}, \tag{1}$$

where $^{\mathrm{T}}$ signifies the transpose of a second-order tensor. For full details of finite deformation theory we refer to the standard text [11].

2.2. Maxwell's static equations for a dielectric

The Eulerian form of the electric field vector is denoted by $\mathbf{E}$ and the associated electric displacement by $\mathbf{D}$. For a quasi-static deformation in the absence of magnetic fields and distributed currents, Maxwell's equations for a dielectric material reduce to

$$\mathrm{curl}\,\mathbf{E} = \mathbf{0}, \quad \mathrm{div}\,\mathbf{D} = 0, \tag{2}$$

which also hold in free space. Here, the curl and div operators relate to the deformed configuration $\mathcal{B}$. The vectors, $\mathbf{D}$ and $\mathbf{E}$ are related by a constitutive equation, details of which are provided in Section 2.3, but in free space they are simply related by $\mathbf{D} = \varepsilon_0\mathbf{E}$, where the constant ε_0 is the electric permittivity of free space.

The boundary conditions associated with (2) have the standard forms

$$\mathbf{n}\times(\mathbf{E}^{\star} - \mathbf{E}) = \mathbf{0}, \quad \mathbf{n}\cdot(\mathbf{D}^{\star} - \mathbf{D}) = \sigma_{\mathrm{f}}, \tag{3}$$

where $\mathbf{E}^{\star}$ and $\mathbf{D}^{\star}$ denote the fields exterior to the material, σ_{f} is the free surface charge per unit area of $\partial\mathcal{B}$ and $\mathbf{n}$ is the unit outward normal to $\partial\mathcal{B}$.

For what follows, it is convenient to introduce the Lagrangian quantities defined by

$$\mathbf{E}_{\mathrm{L}} = \mathbf{F}^{\mathrm{T}}\mathbf{E}, \quad \mathbf{D}_{\mathrm{L}} = \mathbf{F}^{-1}\mathbf{D}, \tag{4}$$

where the subscript $_{\mathrm{L}}$ signifies 'Lagrangian'. The Eulerian field equations (2) can then be written equivalently in Lagrangian form

$$\mathrm{Curl}\,\mathbf{E}_{\mathrm{L}} = \mathbf{0}, \quad \mathrm{Div}\,\mathbf{D}_{\mathrm{L}} = 0, \tag{5}$$

where Curl and Div are the curl and divergence operators with respect to $\mathbf{X}$. These equations are associated with boundary conditions on $\partial\mathcal{B}_{\mathrm{r}}$ analogous to (3), but these will not be used here. For full details we refer to the monograph [12].

2.3. Electroelasticity

A history of the development of the nonlinear theory of continuum electromechanics is summarized in the recent review article [13]. The article describes in some detail the theory of electroelasticity and includes the solution of some representative boundary-value problems. Some details of experiments relating to the large deformation electromechanical effects in elastomeric dielectrics and their use in actuators are also given. Full details of the nonlinear theory of electroelasticity are provided in [14] and [12], while the influence of an electric field on the mechanical response of an incompressible isotropic elastomeric dielectric on the solution of a number of boundary-value problems has been discussed in [15].

2.3.1. Equilibrium equations and boundary conditions

From the general theory [12], the equilibrium equation can be written in the form

$$\mathrm{div}\,\boldsymbol{\tau} + \rho\mathbf{f} = \mathbf{0} \quad \text{in } \mathcal{B}, \tag{6}$$

where $\boldsymbol{\tau}$ is the total Cauchy stress tensor, which is symmetric, ρ is the mass density of the material in the deformed configuration and $\mathbf{f}$ is the mechanical body force per unit mass.

Similarly to the connection between the nominal stress and Cauchy stress in pure elasticity theory, the total nominal stress tensor, denoted $\mathbf{T}$, is defined (for an incompressible material) by $\mathbf{T} = \mathbf{F}^{-1}\boldsymbol{\tau}$, and in terms of $\mathbf{T}$ the equilibrium equation (6) can be written in the equivalent form

$$\mathrm{Div}\,\mathbf{T} + \rho\mathbf{f} = \mathbf{0}, \tag{7}$$

noting that, by incompressibility, ρ is also the density in the reference configuration.

The traction boundary condition associated with the equilibrium equation (6) at a point on $\partial\mathcal{B}$ where the mechanical traction is given has the form

$$\boldsymbol{\tau}\mathbf{n} = \mathbf{t}_{\mathrm{a}} + \mathbf{t}_{\mathrm{m}}^{\star} \quad \text{on } \partial\mathcal{B}, \tag{8}$$

where $\mathbf{t}_{\mathrm{a}}$ is the applied mechanical traction and $\mathbf{t}_{\mathrm{m}}^{\star}$ is the traction due to the exterior electric field given by $\mathbf{t}_{\mathrm{m}}^{\star} = \boldsymbol{\tau}_{\mathrm{m}}^{\star}\mathbf{n}$ in terms of the Maxwell stress tensor $\boldsymbol{\tau}_{\mathrm{m}}^{\star}$ evaluated on the exterior of $\partial\mathcal{B}$ as

$$\boldsymbol{\tau}_{\mathrm{m}}^{\star} = \varepsilon_0\mathbf{E}^{\star}\otimes\mathbf{E}^{\star} - \frac{1}{2}\varepsilon_0\left(\mathbf{E}^{\star}\cdot\mathbf{E}^{\star}\right)\mathbf{I}, \tag{9}$$

where $\mathbf{I}$ is the identity tensor.

The traction boundary condition may also be written in Lagrangian form based on Eq. (7) but it will not be used here. Details are given in [12].

2.3.2. Constitutive equations

A compact way to express constitutive equations in nonlinear electroelasticity is by using either $\mathbf{E}_{\mathrm{L}}$ or $\mathbf{D}_{\mathrm{L}}$ as the independent electric vector variable, and for full details we refer to [14] and [12]. Here we adopt $\mathbf{D}_{\mathrm{L}}$ together with a so-called total electroelastic energy function $\Omega^*(\mathbf{F}, \mathbf{D}_{\mathrm{L}})$, which, by objectivity, depends on $\mathbf{F}$ via the right Cauchy–Green tensor $(1)_1$. The total nominal and Cauchy stress tensors $\mathbf{T}$ and $\boldsymbol{\tau}$ are given by

$$\mathbf{T} = \frac{\partial\Omega^*}{\partial\mathbf{F}} - p^*\mathbf{F}^{-1}, \quad \boldsymbol{\tau} = \mathbf{F}\frac{\partial\Omega^*}{\partial\mathbf{F}} - p^*\mathbf{I}, \tag{10}$$

where p^* is a Lagrange multiplier associated with the incompressibility constraint $\det\mathbf{F} = 1$.

The corresponding expressions for $\mathbf{E}_{\mathrm{L}}$ and $\mathbf{E}$ are

$$\mathbf{E}_{\mathrm{L}} = \frac{\partial\Omega^*}{\partial\mathbf{D}_{\mathrm{L}}}, \quad \mathbf{E} = \mathbf{F}^{-\mathrm{T}}\frac{\partial\Omega^*}{\partial\mathbf{D}_{\mathrm{L}}}. \tag{11}$$

2.3.3. Isotropic electroelasticity

The electroelastic material considered here is said to be *isotropic* if Ω^* is an isotropic function of the two tensors $\mathbf{C}$ and

$\mathbf{D}_\mathrm{L} \otimes \mathbf{D}_\mathrm{L}$, in which case Ω^* depends on five invariants of $\mathbf{C}$ and $\mathbf{D}_\mathrm{L} \otimes \mathbf{D}_\mathrm{L}$, here denoted I_1, I_2, I_4, I_5, I_6 and defined by

$$I_1 = \mathrm{tr}\,\mathbf{C}, \quad I_2 = \frac{1}{2}[I_1^2 - \mathrm{tr}(\mathbf{C}^2)], \tag{12}$$

$$I_4 = \mathbf{D}_\mathrm{L} \cdot \mathbf{D}_\mathrm{L}, \quad I_5 = \mathbf{D}_\mathrm{L} \cdot (\mathbf{C}\mathbf{D}_\mathrm{L}), \quad I_6 = \mathbf{D}_\mathrm{L} \cdot \left(\mathbf{C}^2\mathbf{D}_\mathrm{L}\right). \tag{13}$$

It then follows that

$$\begin{aligned}\boldsymbol{\tau} = 2\Omega_1^*\mathbf{B} \,+\, 2\Omega_2^*\left(I_1 B - \mathbf{B}^2\right) - p^*\mathbf{I} + \,2\Omega_5^*\mathbf{D}\otimes\mathbf{D} \\ +\, 2\Omega_6^*\left(\mathbf{D}\otimes\mathbf{B}\mathbf{D} + \mathbf{B}\mathbf{D}\otimes\mathbf{D}\right),\end{aligned} \tag{14}$$

and

$$\mathbf{E} = 2\left(\Omega_4^*\mathbf{B}^{-1}\mathbf{D} + \Omega_5^*\mathbf{D} + \Omega_6^*\mathbf{B}\mathbf{D}\right), \tag{15}$$

where Ω_i^* defined as $\partial\Omega^*/\partial I_i$ for $i = 1, 2, 4, 5, 6$.

We now write Eq. (15) in the form $\mathbf{D} = \boldsymbol{\varepsilon}\mathbf{E}$, where $\boldsymbol{\varepsilon}$ is the permittivity tensor, which depends on both the deformation and $\mathbf{D}$ in general, and whose inverse can be seen from (15) to be given by

$$\boldsymbol{\varepsilon}^{-1} = 2(\Omega_4^*\mathbf{B}^{-1} + \Omega_5^*\mathbf{I} + \Omega_6^*\mathbf{B}). \tag{16}$$

For the particular model used in [16], we have $\Omega_4^* = \varepsilon_0^{-1}\alpha/2$, $\Omega_5^* = \varepsilon_0^{-1}\beta/2$, $\Omega_6^* = 0$, where α and β are dimensionless constants, and (16) becomes

$$\boldsymbol{\varepsilon}^{-1} = \varepsilon_0^{-1}(\alpha\mathbf{B}^{-1} + \beta\mathbf{I}). \tag{17}$$

Note that if $\alpha = 0$ then $\beta^{-1} = \varepsilon/\varepsilon_0$ is the constant relative permittivity of a material with isotropic dielectric properties.

3. Application to a thick-walled tube

Having established the constitutive law in terms of a Lagrangian variable, it is convenient for the problem considered below to use the expressions for the Eulerian fields given in (14) and (15) and to ensure that Eqs. (2) and (6) are satisfied.

3.1. Combined extension, inflation and torsion

We now apply the foregoing theory to the deformation consisting of axial extension, radial inflation and torsion of a thick-walled circular cylindrical tube, the underlying theory for which has been well known since the seminal contributions of Rivlin [17, 18]. Here we summarize the main ingredients of the theory ready for the incorporation of a radial electric field in the following subsection. We note in passing that for a piezoelectric material in the presence of a radial electric field this deformation was first examined in [19] in the context of a study of controllable deformations.

The reference geometry of the tube is described in terms of cylindrical polar coordinates (R, Θ, Z), associated with unit basis vectors $\mathbf{E}_R, \mathbf{E}_\Theta, \mathbf{E}_Z$, by

$$0 < A \le R \le B, \quad 0 \le \Theta \le 2\pi, \quad 0 \le Z \le L, \tag{18}$$

where A and B are the internal and external radii and L is the length of the tube. The position vector $\mathbf{X}$ of a point of the tube is given by $\mathbf{X} = R\mathbf{E}_R + Z\mathbf{E}_Z$.

The corresponding deformed geometry is defined by

$$a \le r \le b, \quad 0 \le \theta \le 2\pi, \quad 0 \le z \le l \tag{19}$$

in terms of cylindrical polar coordinates (r, θ, z) associated with unit basis vectors $\mathbf{e}_r, \mathbf{e}_\theta, \mathbf{e}_z$, the position vector $\mathbf{x}$ in the deformed tube is written $\mathbf{x} = r\mathbf{e}_r + z\mathbf{e}_z$, and the deformation is defined by

$$r = f(R) \equiv \sqrt{a^2 + \lambda_z^{-1}(R^2 - A^2)}, \quad \theta = \Theta + \psi\lambda_z Z, \quad z = \lambda_z Z, \tag{20}$$

in which the first term results from incompressibility, λ_z is the (uniform) axial stretch, and the constant ψ is the torsion per unit deformed length of the tube. Note that $b = f(B)$ and $l = \lambda_z L$.

The associated deformation gradient tensor $\mathbf{F}$ takes the form

$$\mathbf{F} = \lambda_r\,\mathbf{e}_r\otimes\mathbf{E}_R + \lambda_\theta\,\mathbf{e}_\theta\otimes\mathbf{E}_\Theta + \lambda_z\,\mathbf{e}_z\otimes\mathbf{E}_Z + \lambda_z\gamma\,\mathbf{e}_\theta\otimes\mathbf{E}_Z, \tag{21}$$

where the notation γ is defined as $\gamma = \psi r$, while $\lambda_\theta = r/R$ and, by incompressibility, $\lambda_r = \lambda_\theta^{-1}\lambda_z^{-1}$. The deformation tensors (1) specialize to

$$\begin{aligned}\mathbf{C} &= \lambda_r^2\mathbf{E}_R\otimes\mathbf{E}_R + \lambda_\theta^2\mathbf{E}_\Theta\otimes\mathbf{E}_\Theta + \lambda_z^2(1+\gamma^2)\mathbf{E}_Z\otimes\mathbf{E}_Z \\ &\quad + \gamma\lambda_z\lambda_\theta(\mathbf{E}_\Theta\otimes\mathbf{E}_Z + \mathbf{E}_Z\otimes\mathbf{E}_\Theta), \\ \mathbf{B} &= \lambda_r^2\mathbf{e}_r\otimes\mathbf{e}_r + (\lambda_\theta^2 + \gamma^2\lambda_z^2)\mathbf{e}_\theta\otimes\mathbf{e}_\theta + \lambda_z^2\mathbf{e}_z\otimes\mathbf{e}_z \\ &\quad + \gamma\lambda_z^2(\mathbf{e}_\theta\otimes\mathbf{e}_z + \mathbf{e}_z\otimes\mathbf{e}_\theta).\end{aligned} \tag{22}$$

3.2. Electric field components and boundary conditions

Flexible electrodes are affixed to the surfaces $R = A$ and $R = B$ across which is applied a potential difference, accompanied by equal and opposite charges on the electrodes totalling Q and $-Q$, respectively. Then, by Gauss's theorem, no field is generated outside the tube, assuming that the geometry is such that end effects can be neglected.

For this problem the independent Lagrangian electric displacement field $\mathbf{D}_\mathrm{L}$ has only a radial component $D_R = D_R(R)$, a function of R only, and, by $(4)_2$, the corresponding Eulerian field has only the single component $D_r(r)$, which is given by $D_r = \lambda_r D_R$. Equation (2) then reduces to $\mathrm{d}(rD_r)/\mathrm{d}r = 0$, so that $rD_r(r)$ is constant, and hence $rD_r(r) = aD_r(a) = bD_r(b)$. With reference to the boundary condition $(3)_2$, the surface charge per unit deformed area is $Q/(2\pi al)$, and hence $D_r(a) = Q/(2\pi al)$ and

$$D_r(r) = \frac{Q}{2\pi rl}. \tag{23}$$

The invariants defined in (12) and (13) specialize to

$$I_1 = \lambda_z^{-2}\lambda_\theta^{-2} + \lambda_\theta^2 + \lambda_z^2(1+\gamma^2), \quad I_2 = \lambda_z^2\lambda_\theta^2 + \lambda_\theta^{-2}(1+\gamma^2) + \lambda_z^{-2}, \tag{24}$$

and

$$I_4 = D_R^2 = \lambda_\theta^2\lambda_z^2 D_r^2, \quad I_5 = \lambda_\theta^{-2}\lambda_z^{-2}I_4, \quad I_6 = \lambda_\theta^{-4}\lambda_z^{-4}I_4. \tag{25}$$

From (15) it follows that $\mathbf{E}$ has only a radial component, $E_r(r)$, which is given by

$$E_r = 2\left(\Omega_4^*\lambda_\theta^2\lambda_z^2 + \Omega_5^* + \Omega_6^*\lambda_\theta^{-2}\lambda_z^{-2}\right)D_r, \tag{26}$$

and Eq. $(2)_1$ is automatically satisfied.

3.3. Specialization of the constitutive equations and mechanical equilibrium

The components of the total Cauchy stress tensor are now obtained by specializing Eq. (14) to obtain $\tau_{r\theta} = \tau_{rz} = 0$,

$$\tau_{rr} = 2\Omega_1^*\lambda_\theta^{-2}\lambda_z^{-2} + 2\Omega_2^*\left(\left(1+\gamma^2\right)\lambda_\theta^{-2} + \lambda_z^{-2}\right) - p^* + 2\Omega_5^* D_r^2 + 4\Omega_6^*\lambda_\theta^{-2}\lambda_z^{-2}D_r^2, \quad (27)$$

$$\tau_{\theta\theta} = 2\Omega_1^*(\lambda_\theta^2 + \gamma^2\lambda_z^2) + 2\Omega_2^*\left(\lambda_\theta^2\lambda_z^2 + \gamma^2\lambda_\theta^{-2} + \lambda_z^{-2}\right) - p^*, \quad (28)$$

$$\tau_{zz} = 2\Omega_1^*\lambda_z^2 + 2\Omega_2^*\left(\lambda_\theta^2\lambda_z^2 + \lambda_\theta^{-2}\right) - p^*, \quad (29)$$

$$\tau_{\theta z} = 2\Omega_1^*\gamma\lambda_z^2 + 2\Omega_2^*\gamma\lambda_\theta^{-2}. \quad (30)$$

The invariants (24) and (25) depend on three independent deformation variables λ_θ, λ_z and γ, together with I_4. It is therefore convenient to introduce a reduced energy function, denoted ω^* and defined by

$$\omega^*(\lambda_\theta, \lambda_z, \gamma, I_4) = \Omega^*(I_1, I_2, I_4, I_5, I_6), \quad (31)$$

where, on the right-hand side, the invariants are given by (24) and (25). A straightforward calculation based on Eqs. (27)–(30) leads to

$$\tau_{\theta\theta} - \tau_{rr} = \lambda_\theta\frac{\partial\omega^*}{\partial\lambda_\theta} + \gamma\frac{\partial\omega^*}{\partial\gamma}, \quad \tau_{zz} - \tau_{rr} = \lambda_z\frac{\partial\omega^*}{\partial\lambda_z} - \gamma\frac{\partial\omega^*}{\partial\gamma}, \quad \tau_{\theta z} = \frac{\partial\omega^*}{\partial\gamma}, \quad (32)$$

Similarly, in terms of ω^*, Eq. (26) simplifies to

$$E_r = 2\lambda_\theta^2\lambda_z^2\frac{\partial\omega^*}{\partial I_4}D_r. \quad (33)$$

Because of the radial symmetry, the equilibrium equation (6) in the absence of mechanical body forces specializes to the single (radial) component

$$r\frac{\mathrm{d}\tau_{rr}}{\mathrm{d}r} = \tau_{\theta\theta} - \tau_{rr}. \quad (34)$$

There is no electric field outside the tube, and hence no Maxwell stress, and any traction on $r = a$ and $r = b$ is purely due to applied mechanical loads. We assume that there is no such load on $r = b$ and that the load on $r = a$ is due to an internal pressure P (per unit area). Thus, $\tau_{rr} = -P$ and 0 on $r = a$ and $r = b$, respectively. Integration of (34) after substitution from $(32)_1$ then leads to

$$P = \int_a^b \left(\lambda_\theta\frac{\partial\omega^*}{\partial\lambda_\theta} + \gamma\frac{\partial\omega^*}{\partial\gamma}\right)\frac{\mathrm{d}r}{r}. \quad (35)$$

The shear stress $\sigma_{\theta z}$ generates a torsional moment M on any cross section of the tube, which, on use of $(32)_3$, is given by

$$M = 2\pi\int_a^b \tau_{\theta z}r^2\mathrm{d}r = 2\pi\int_a^b \frac{\partial\omega^*}{\partial\gamma}r^2\mathrm{d}r. \quad (36)$$

An axial load is also generated. For a tube with closed ends, after removal of the effect of P on the ends, the resultant, denoted F, is known as the reduced axial load, which, by a standard calculation and use of (32), has the form

$$F = \pi\int_a^b (2\tau_{zz} - \tau_{rr} - \tau_{\theta\theta})\, r\mathrm{d}r = \pi\int_a^b \left(2\lambda_z\frac{\partial\omega^*}{\partial\lambda_z} - \lambda_\theta\frac{\partial\omega^*}{\partial\lambda_\theta} - 3\gamma\frac{\partial\omega^*}{\partial\gamma}\right)r\mathrm{d}r. \quad (37)$$

In the following two sections, for purposes of illustration, we consider the energy function $\omega^*(\lambda_\theta, \lambda_z, \gamma, I_4)$ to be decomposed in the form

$$\omega^*(\lambda_\theta, \lambda_z, \gamma, I_4) = \omega_\mathrm{m}(\lambda_\theta, \lambda_z, \gamma) + \omega_\mathrm{e}(\lambda_\theta, \lambda_z, \gamma, I_4), \quad (38)$$

where ω_m is a purely mechanical (elastic) energy function and ω_e is the energy associated with the electric field, which may in general also depend on the deformation. Both functions will be specialized in the next two sections.

4. Application to the neo-Hookean model

In this section we assume that ω_m is given as the neo-Hookean model, so that

$$\omega_\mathrm{m} = \frac{1}{2}\mu(I_1 - 3) = \frac{1}{2}\mu\left[\lambda_\theta^{-2}\lambda_z^{-2} + \lambda_\theta^2 + \lambda_z^2(1+\gamma^2) - 3\right], \quad (39)$$

where the constant $\mu\,(>0)$ is the shear modulus of the material in the reference configuration.

4.1. Deformation dependent permittivity

For the electric contribution we first consider the isotropic constitutive law with constant permittivity ε, i.e. $\mathbf{D} = \varepsilon\mathbf{E}$, for which the electrostatic energy is $\mathbf{D}\cdot\mathbf{D}/(2\varepsilon)$, or in terms of $\mathbf{D}_\mathrm{L}$, $\mathbf{D}_\mathrm{L}\cdot(\mathbf{C}\mathbf{D}_\mathrm{L})/(2\varepsilon)$. For the present situation this becomes $\lambda_r^2 D_R^2/(2\varepsilon)$, and hence

$$\omega_\mathrm{e} = \frac{1}{2\varepsilon}\lambda_\theta^{-2}\lambda_z^{-2}I_4. \quad (40)$$

In respect of the more general expression (17) this is replaced by

$$\omega_\mathrm{e} = \frac{1}{2\varepsilon_0}(\alpha + \beta\lambda_\theta^{-2}\lambda_z^{-2})I_4, \quad (41)$$

where $\alpha\,(>0)$ is a measure of the deformation dependence of the permittivity, while $\beta\,(>0)$ becomes $\varepsilon_0/\varepsilon$ when $\alpha = 0$. Note that evaluation in the reference configuration gives the relative permittivity $1/(\alpha+\beta)$, which must be greater than 1 for all electro-active materials, as noted in [16]. Thus, $\alpha+\beta < 1$ for this model, which was introduced in [16] to reflect the experimental evidence noted in, for example, [2, 3] that the permittivity of a thin film of dielectric elastomer decreases as the thickness of the film decreases, i.e. as the strain increases.

The expression (41) does not include any dependence on γ, and it therefore needs to be modified if such a dependence turns out to be necessary. For such an eventuality we now consider the α term to depend on $I_1 = \lambda_\theta^{-2}\lambda_z^{-2} + \lambda_\theta^2 + \lambda_z^2(1+\gamma^2)$ in the form

$$\omega_\mathrm{e} = \frac{1}{2\varepsilon_0}[\alpha(I_1 - 3) + \beta\lambda_\theta^{-2}\lambda_z^{-2}]I_4, \quad (42)$$

noting that $I_1 \geq 3$, with equality holding only in the undeformed configuration. In the undeformed configuration the relative permittivity becomes β^{-1} and we must have $\beta < 1$ for this model, but no immediate restriction is placed on α in this case.

4.2. Pressure, moment and axial force

To evaluate the integrals for P, M and F in (35), (36) and (37), respectively, in respect of (39) and (42) the expressions

$$\lambda_\theta \frac{\partial \omega^*}{\partial \lambda_\theta} = \mu\left(\lambda_\theta^2 - \lambda_\theta^{-2}\lambda_z^{-2}\right) - \varepsilon_0^{-1}\left[\alpha\lambda_\theta^2 - (\alpha+\beta)\lambda_\theta^{-2}\lambda_z^{-2}\right] I_4, \quad (43)$$

$$\lambda_z \frac{\partial \omega^*}{\partial \lambda_z} = \mu\left[\lambda_z^2\left(1+\gamma^2\right) - \lambda_\theta^{-2}\lambda_z^{-2}\right] - \varepsilon_0^{-1}\left[\alpha\lambda_z^2(1+\gamma^2) - (\alpha+\beta)\lambda_\theta^{-2}\lambda_z^{-2}\right] I_4, \quad (44)$$

$$\gamma \frac{\partial \omega^*}{\partial \gamma} = (\mu + \varepsilon_0^{-1}\alpha I_4)\lambda_z^2\gamma^2, \quad (45)$$

are needed. We also note that, as required for (33),

$$\frac{\partial \omega^*}{\partial I_4} = \frac{1}{2\varepsilon_0}\left[\alpha(I_1 - 3) + \beta\lambda_\theta^{-2}\lambda_z^{-2}\right]. \quad (46)$$

It is now convenient to decompose the expressions for P, M and F as

$$P = P_\mathrm{m} + P_\mathrm{e}, \quad M = M_\mathrm{m} + M_\mathrm{e}, \quad F = F_\mathrm{m} + F_\mathrm{e} \quad (47)$$

in respect of their contributions from ω_m and ω_e. With the help of (43)–(45), the definitions $\gamma = \psi r$, $\lambda_\theta = r/R$, $I_4 = D_R^2$, with $D_R = Q/(2\pi LR)$, and Eq. (20), each expression in (47) can be integrated explicitly. For this purpose we introduce the notation

$$q = \left(\frac{Q}{2\pi AL}\right)^2, \quad (48)$$

so that $I_4 = qA^2/R^2$. We also use the notations defined by $\eta = B/A$, $\psi^* = \psi A$, $\lambda_a = a/A$ and $\lambda_b = b/B$, with the connection $\lambda_b^2 = [\lambda_a^2 + (\eta^2 - 1)/\lambda_z]/\eta^2$, which is obtained from $(20)_1$ with $b = f(B)$.

First, we obtain

$$P_\mathrm{m} = \frac{\mu}{2}\left[\frac{2}{\lambda_z}\log\left(\frac{\lambda_a}{\lambda_b}\right) + \lambda_z\psi^{*2}\left(\eta^2 - 1\right) - \frac{\left(\eta^2-1\right)\left(1 - \lambda_a^2\lambda_z\right)}{\eta^2\lambda_z^3\lambda_a^2\lambda_b^2}\right], \quad (49)$$

$$P_\mathrm{e} = \frac{q}{2\varepsilon_0}\left[\alpha\frac{\eta^2-1}{\lambda_z\eta^2} - (\alpha+\beta)\frac{\eta^2-1}{\lambda_z^3\lambda_a^2\lambda_b^2} + 2\alpha\lambda_z\psi^{*2}\log\eta\right]. \quad (50)$$

Next,

$$M_\mathrm{m} = \frac{1}{2}\pi\mu\psi^*\lambda_z A^3\left(\lambda_a^2 + \lambda_b^2\eta^2\right)\left(\eta^2 - 1\right), \quad (51)$$

$$M_\mathrm{e} = \frac{1}{\varepsilon_0}\pi\alpha q\psi^* A^3[2(\lambda_a^2\lambda_z - 1)\log\eta + \eta^2 - 1]. \quad (52)$$

Finally,

$$F_\mathrm{m} = \pi\mu A^2\left[\left(\lambda_z - \lambda_z^{-2}\right)\left(\eta^2-1\right) - \lambda_z^{-2}\left(\lambda_a^2\lambda_z - 1\right)\log\left(\frac{\lambda_a}{\lambda_b}\right) - \frac{1}{4}\lambda_z\psi^{*2}\left(\eta^2-1\right)\left(\lambda_a^2 + \eta^2\lambda_b^2\right)\right], \quad (53)$$

$$F_\mathrm{e} = \pi A^2\frac{q}{\varepsilon_0}\left\{\left[2\alpha(\lambda_z - \lambda_z^{-2}) - \beta\lambda_z^{-2}\right]\log\eta - \tfrac{1}{2}\alpha\lambda_z^{-2}(\lambda_a^2\lambda_z - 1)\frac{\eta^2-1}{\eta^2} + (\alpha+\beta)\lambda_z^{-2}\log\left(\frac{\lambda_a}{\lambda_b}\right) - \tfrac{1}{2}\alpha\psi^{*2}\left[\eta^2 - 1 + 2(\lambda_a^2\lambda_z - 1)\log\eta\right]\right\}. \quad (54)$$

Note that equivalent expressions for the elastic parts of P and F were given in [1] for the case $\psi^* = 0$.

From Eq. $(2)_1$ it follows that $\mathbf{E} = -\mathrm{grad}\,\phi$, where the scalar field ϕ is known as the electrostatic potential. In the present context this has only a radial component $E_r = -\mathrm{d}\phi/\mathrm{d}r$, and hence, by (33),

$$\frac{\mathrm{d}\phi}{\mathrm{d}r} = -2\lambda_\theta^2\lambda_z^2\frac{\partial\omega^*}{\partial I_4}D_r, \quad (55)$$

which, on integration and substitution from (46) and (23), gives the potential difference between the electrodes as

$$\phi(b) - \phi(a) = -\frac{Q}{2\pi\varepsilon_0 l}\int_a^b\left[\alpha(I_1 - 3)\lambda_\theta^2\lambda_z^2 + \beta\right]\frac{\mathrm{d}r}{r}. \quad (56)$$

Integration results in the connection between q and the potential difference and yields

$$\phi(b) - \phi(a) = -\frac{\sqrt{q}A}{\varepsilon_0\lambda_z}\left\{(\alpha+\beta)\log\left(\frac{\eta\lambda_b}{\lambda_a}\right) + \alpha\left[(\lambda_z^3 - 3\lambda_z + 1)\log\eta + \frac{1}{2}(\lambda_a^2\lambda_z - 1)\frac{\eta^2-1}{\eta^2} + (\lambda_a^2\lambda_z - 1)\lambda_z^2\psi^{*2}\log\eta + \frac{1}{2}\lambda_z^2\psi^{*2}(\eta^2-1)\right]\right\} = -\frac{\sqrt{q}A}{\varepsilon_0\lambda_z}s, \quad (57)$$

where the shorthand notation s is introduced to represent the term enclosed by the curly brackets.

The notation E_0 is now used for the mean value of the electric field. It is given by

$$E_0 = \frac{\phi(b) - \phi(a)}{B - A}, \quad (58)$$

which is a measure of the potential difference, related to q by

$$q = \frac{\varepsilon_0^2 E_0^2\lambda_z^2(\eta-1)^2}{s^2}, \quad (59)$$

a particular case of which corresponding to deformation independent permittivity was derived in [1]. From this connection, q in the expressions for P_e, M_e and F_e in (50), (52) and (54), which define their dependence on the charge, can be replaced by E_0 to determine their dependence on the potential difference.

4.3. Numerical illustrations

To illustrate the results it is convenient to define the following additional dimensionless quantities:

$$P^* = \frac{P}{\mu}, \quad F^* = \frac{F}{\pi\mu A^2}, \quad M^* = \frac{M}{\pi\mu A^3}, \quad (60)$$

$$q^* = \frac{q}{\mu\varepsilon_0}, \quad e^* = \frac{\varepsilon_0 E_0^2}{\mu}. \quad (61)$$

The dielectric parameters in (42) are taken to have the representative values $\alpha = 0.25$ and $\beta = 0.5$ in all the examples.

Figure 1 shows the dependence of the dimensionless form of the pressure P^* on the stretch λ_a for a tube with $\eta = B/A = 1.3$ and fixed axial stretch $\lambda_z = 1.2$. Results are obtained from (49) and (50) with $P = P_{\rm m} + P_{\rm e}$ for fixed values of $\psi^* = 0, 0.5, 1$ (the first, second and third rows, respectively). In each panel of the left-hand column the plots are for $q^* = 0, 5, 10, 20$, and in the right-hand column for $e^* = 0, 5, 10, 20$, in each case depicted by the continuous, dashed, dotted and dashed-dotted curves, respectively.

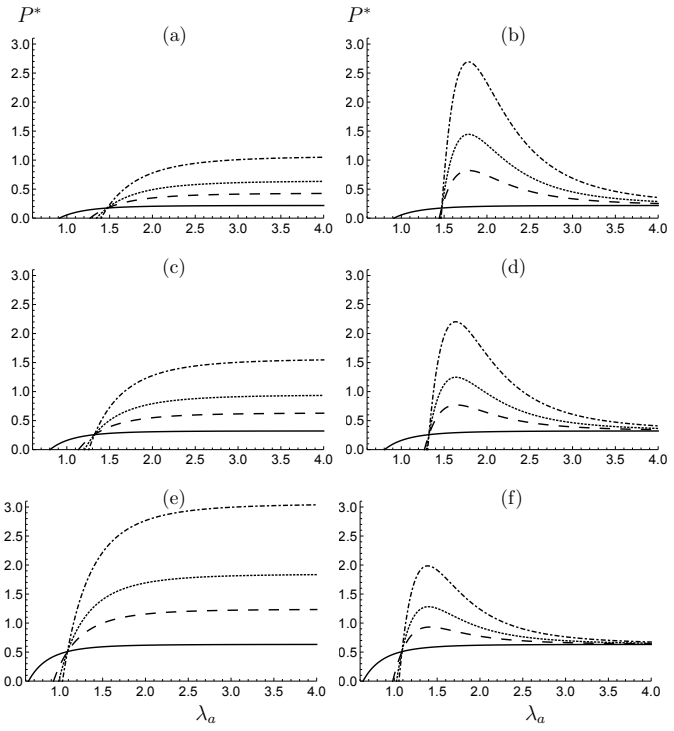

Figure 1: Plots of the dimensionless pressure P^* as a function of the stretch λ_a for a neo-Hookean dielectric with deformation dependent permittivity. Plots for $q^* = 0, 5, 10, 20$ (left-hand column) and $e^* = 0, 5, 10, 20$ (right-hand column) are depicted by continuous, dashed, dotted and dashed-dotted curves, respectively, in each panel. Panels (a) and (b) are for the case with no torsion ($\psi^* = 0$); panels (c) and (d) correspond to $\psi^* = 0.5$; for panels (e) and (f), $\psi^* = 1$.

The continuous curves, which correspond to $q^* = 0$ or $e^* = 0$, represent the purely elastic responses and they coincide for each value of ψ^*. When $\psi^* = 0$, since λ_z is fixed at 1.2, inflation is initiated at $P^* = 0$ with $\lambda_a < 1$, but an increase in ψ^* when $P^* = 0$ reduces the value of λ_a and therefore requires a higher pressures to inflate the tube to the same radius as for $\psi^* = 0$.

The dependence of P^* on the charge density via q^* is illustrated in the left-hand column. At $P^* = 0$ the inner radius increases with q^*, the increase being largest in the absence of any torsion (as measured by ψ^*). As in the mechanical case, an applied torsion requires higher pressures for a given λ_a. Note that, unlike the situation with a constant permittivity for $\psi^* = 0$ [1], the pressure does not tend to the elastic value, independently of q^*, with increasing values of λ_a.

In the right-hand column, on use of the connection (59) to switch from q^* to e^*, the corresponding dependence of P^* on the potential difference via e^* is shown. As for q^*, with $P^* = 0$, increasing values of e^* induce increases in λ_a, but slightly less so than for q^*. Again, as for the left-hand column, increasing values of ψ^* require larger inflation pressures. However, with increasing λ_a the pressure converges to the purely elastic value independently of e^*, in contrast to the case of constant permittivity for $\psi^* = 0$ [1]. It is of interest to observe that in each panel of Fig. 1 the curves all intersect at the same point (which is different for each panel). The appropriate value of λ_a is given by a solution of $P_{\rm e} = 0$ independently of q^* (or e^*) since $P_{\rm m}$ is the same for each such q^* (or e^*). This means that such a λ_a is given by $s = 0$, where s is defined in (57).

The case of constant permittivity is recovered by taking $\alpha = 0$. The curve for $q^* = 0$ (or $e^* = 0$) in Fig. 1 is the same as that obtained for $\alpha = 0$, while for non-zero q^* (or e^*) the corresponding curves are similar to this one. For each different value of q^* (or e^*) they start with a different value of $\lambda_a > 1$ for $P^* = 0$, then increase monotonically, but remain below it and asymptote to it as λ_a increases.

Note that for the $e^* \neq 0$ plots in Fig. 1 a maximum is induced in the pressure. This is associated with an instability, as discussed in some detail in [1] and references therein. A similar comment applies to the plots of the torsional moment in Fig. 2, although in this case the maximum is phased out as ψ^* increases. The results for the Gent model shown later in Figs. 4 and 5, have similar interpretation, except that, by contrast with the neo-Hookean based model, the upturn is associated with the possibility of a snap-through instability.

In Fig. 2 the dependence of the dimensionless torsional moment M^* on the dimensionless torsional strain ψ^* is illustrated, again with $\eta = B/A = 1.3$ and $\lambda_z = 1.2$. Reading from top to bottom, the three rows correspond to fixed values of λ_a, specifically $1, 1.5, 2.5$, respectively. In each panel of the left-hand column the plots are for $q^* = 0, 5, 10, 20$, and in the right-hand column for $e^* = 0, 5, 10, 20$, in each case depicted by the continuous, dashed, dotted and dashed-dotted curves, respectively. It is clear from (51) and (52) that for fixed q^* and λ_a with $M = M_{\rm m} + M_{\rm e}$ the torsional response is linear and becomes stiffer as q^* increases. On the other hand, for fixed e^*, the right-hand column shows that the response is highly nonlinear and approaches the purely elastic result as ψ^* increases. If the permittivity is constant ($\alpha = 0$) then $M = M_{\rm m}$ and the relevant plots are the continuous straight lines in Fig. 2.

The four panels in the left-hand column of Fig. 3 show the dependence of the dimensionless axial force F^* on λ_a, again with $\eta = B/A = 1.3$ and $\lambda_z = 1.2$, based on $F = F_{\rm m} + F_{\rm e}$, with (53) and (54). The panels in Fig. 3 are arranged as for Fig. 1 with the same values of the parameters q^*, e^* and ψ^*. Positive (negative) values of F^* correspond to tension (compression), which would be needed to maintain the tube length and prevent it shortening (lengthening). The plots for $q^* = 0, 5, 10, 20$ (left-hand column) and for $e^* = 0, 5, 10, 20$ (right-hand column) correspond to the continuous, dashed, dotted and dashed-dotted curves, respectively, in each case.

In the absence of an electric field, with $\psi^* = 0$ and $P^* = 0$, a slightly positive value of F^* supports the axial stretch $\lambda_z = 1.2$,

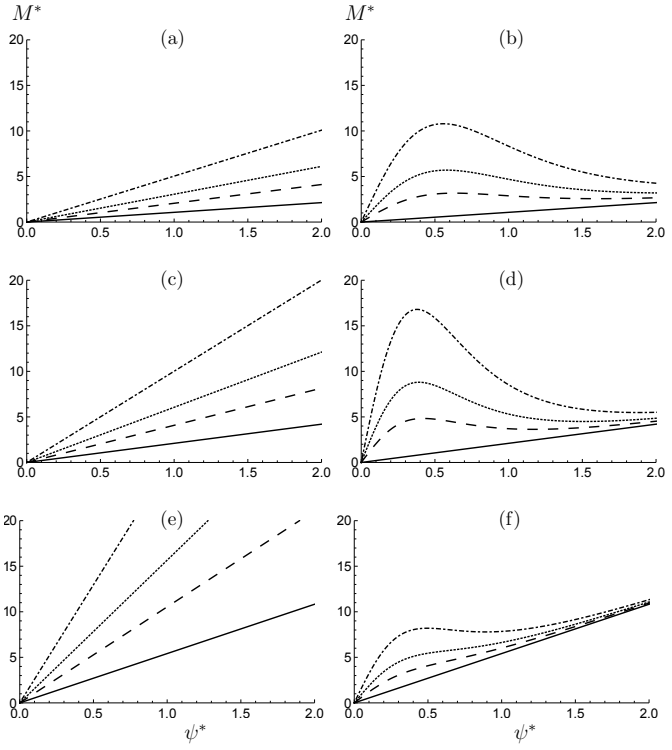

Figure 2: Plots of the dimensionless moment M^* as a function of the dimensionless torsion ψ^* for a neo-Hookean dielectric with deformation dependent permittivity. Curves for $q^* = 0, 5, 10, 20$ (left-hand column) and $e^* = 0, 5, 10, 20$ (right-hand column) are depicted by continuous, dashed, dotted and dashed-dotted curves, respectively, in each panel. Panels (a) and (b) are for the case with $\lambda_a = 1$; panels (c) and (d) correspond to $\lambda_a = 1.5$; for panels (e) and (f), $\lambda_a = 2.5$.

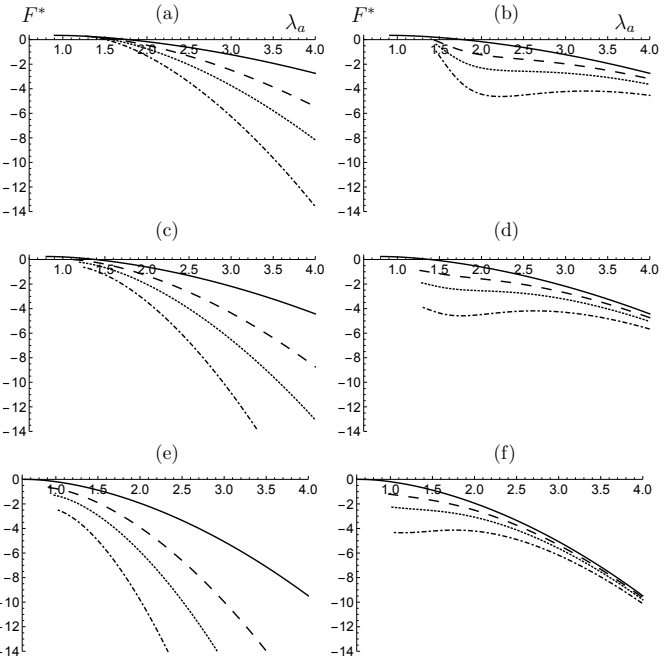

Figure 3: Plots of the dimensionless reduced axial force F^* as a function of the stretch λ_a for a neo-Hookean dielectric with deformation dependent permittivity. Curves for $q^* = 0, 5, 10, 20$ (left-hand column) and $e^* = 0, 5, 10, 20$ (right-hand column) are depicted by continuous, dashed, dotted and dashed-dotted curves, respectively, in each panel. Panels (a) and (b) are for the case with no torsion ($\psi^* = 0$); panels (c) and (d) correspond to $\psi^* = 0.5$; for panels (e) and (f), $\psi^* = 1$.

but, with increasing values of λ_a, F^* becomes negative and decreases monotonically. This transition from positive to negative F^* is advanced as ψ^* increases from 0, and more so when a charge or potential is applied, and then F^* becomes negative for all relevant values of λ_a. The results in the left-hand column are qualitatively similar to those in the purely elastic case and for the case with $\psi^* = 0$ and constant permittivity [1] except that F^* here (for different q^*s) does not converge to the purely elastic solution as λ_a increases.

The results in the right-hand column have some different features. In particular, F^* is not a monotonic function of λ_a for every combination of e^* and ψ^* values and, for each value of e^*, F^* tends to the purely elastic solution with increasing λ_a, both these being in contrast to the results for $\psi^* = 0$ with constant permittivity.

It is clear from Figs. 1–3 that deformation dependent permittivity (through the parameter α) has a significant effect on the material response, even on the basis of the simple neo-Hookean elastic model. This model, it should be emphasized, provides an accurate reflection of the behaviour of rubberize elasticity only for moderate deformations, as is well known, and this is evidenced by the fact that the pressure tends to a finite value as λ_a increases indefinitely. The model does not account for the material stiffening observed experimentally at large deformations. A more realistic model that accounts for such a stiffening in the large deformation regime is that of Gent [8]. The following section therefore uses this model for the elastic part $\omega_{\rm m}$ of the energy function ω^*, together with the electric part $\omega_{\rm e}$ used in Section 4.

5. Application to the Gent model

For the Gent model [8] $\omega_{\rm m}$ is given by

$$\omega_{\rm m} = -\frac{\mu G}{2}\log\left[1 - \frac{\lambda_\theta^2 + \lambda_z^2(1+\gamma^2) + \lambda_\theta^{-2}\lambda_z^{-2} - 3}{G}\right], \qquad (62)$$

where μ is again the shear modulus in the undeformed configuration and G is a dimensionless material constant. The elastic contributions to P, M and F in (49), (51) and (53) are now evaluated numerically using Mathematica [20], while the electric contributions are again given explicitly by (50), (52) and (54). In the following illustrations G is taken to have the representative value 45, again with $\eta = 1.3$, $\lambda_z = 1.2$ and dielectric parameters $\alpha = 0.25$ and $\beta = 0.5$.

In Fig. 4 the dimensionless pressure P^* is plotted as a function of λ_a for $\psi^* = 0, 0.5, 1$, corresponding to the three rows of panels, as for the neo-Hookean model. Comparing the results in Fig. 4 with those Fig. 1 we observe that the initial parts of the responses for moderate values of λ_a are very similar for all values of q^* and e^*, and the discussion in Section 4 therefore still applies and is not be repeated here. The main difference between the predictions of the neo-Hookean and Gent models

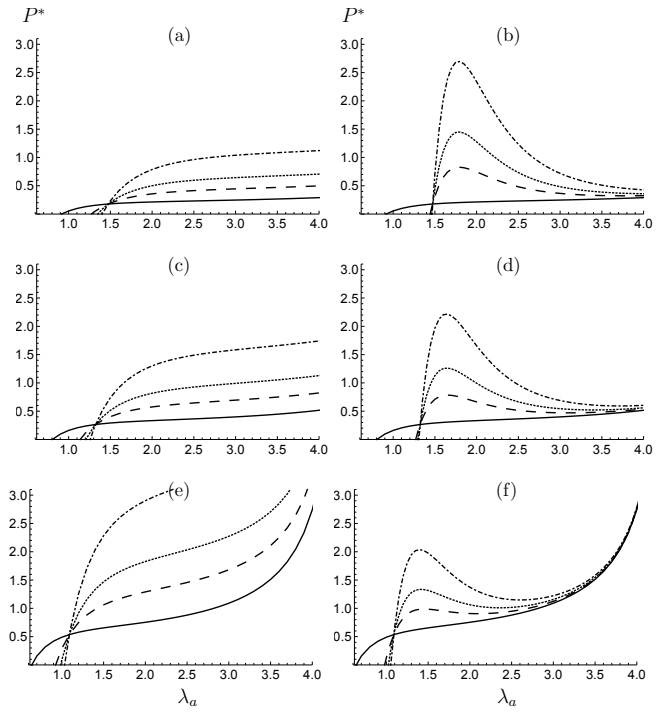

Figure 4: Plots of the dimensionless pressure P^* as a function of the stretch λ_a for a Gent dielectric with deformation dependent permittivity. Plots for $q^* = 0, 5, 10, 20$ (left-hand column) and $e^* = 0, 5, 10, 20$ (right-hand column) are depicted by continuous, dashed, dotted and dashed-dotted curves, respectively, in each panel. Panels (a) and (b) are for the case with no torsion ($\psi^* = 0$); panels (c) and (d) correspond to $\psi^* = 0.5$; for panels (e) and (f), $\psi^* = 1$.

is that for the latter the response stiffens significantly for large deformations as λ_a approaches its asymptotic value defined by $I_1 = 3 + G$ in (62).

Figure 5 shows the torsional behaviour of the Gent model with M^* plotted against ψ^*. In this case the three rows correspond to fixed values of λ_a, namely $1, 1.5, 2.5$. In each panel of the left-hand column the curves are for $q^* = 0, 5, 10, 20$ and in the right-hand column for $e^* = 0, 5, 10, 20$, in each case corresponding to the continuous, dashed, dotted and dashed-dotted curves, respectively. The main differences compared with the neo-Hookean plots are the stiffening at larger values of ψ^* and the nonlinearity in some of the q^* plots for the Gent model compared with the linear neo-Hookean results.

Qualitatively, the results for F^* against λ_a shown in Fig. 6 are similar to those for the neo-Hookean model, but again the response stiffens more rapidly as λ_a increases than for the neo-Hookean model.

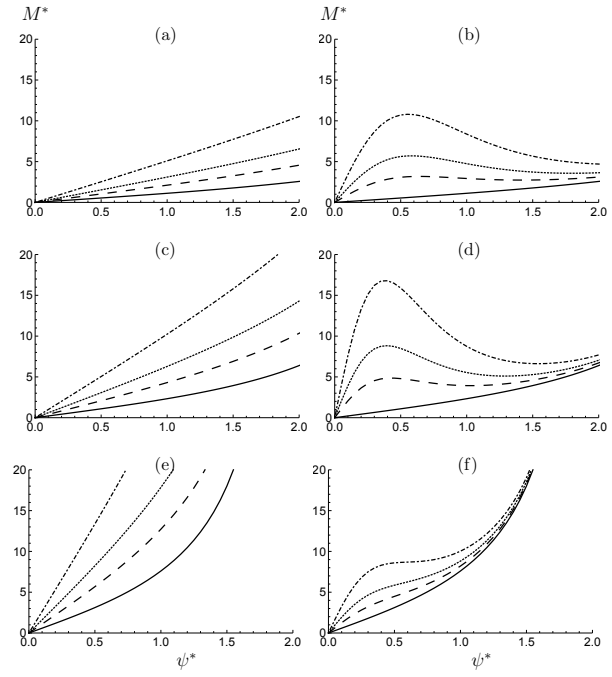

Figure 5: Plots of the dimensionless moment M^* as a function of the dimensionless torsional strain ψ^* for a Gent dielectric with deformation dependent permittivity. Curves for $q^* = 0, 5, 10, 20$ (left-hand column) and $e^* = 0, 5, 10, 20$ (right-hand column) are depicted by continuous, dashed, dotted and dashed-dotted curves, respectively, in each panel. Panels (a) and (b) are for the case with $\lambda_a = 1$; panels (c) and (d) correspond to $\lambda_a = 1.5$; for panels (e) and (f), $\lambda_a = 2.5$.

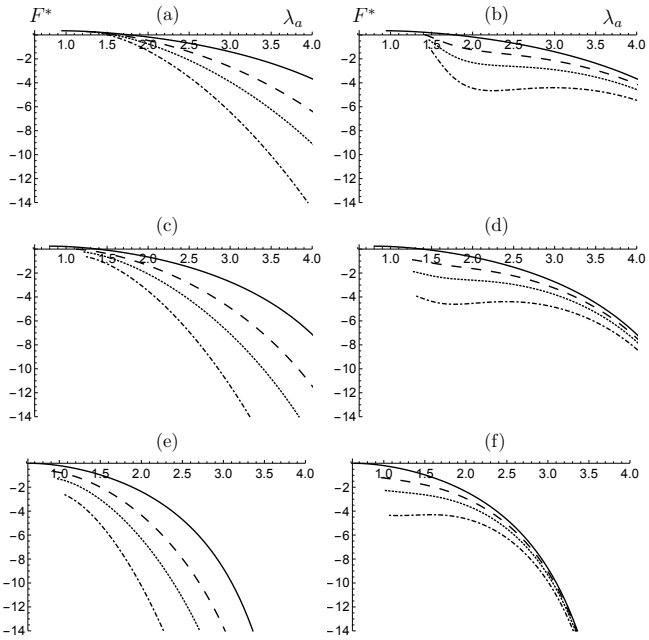

Figure 6: Plots of the dimensionless reduced axial force F^* as a function of the stretch λ_a for a Gent dielectric with deformation dependent permittivity. Curves for $q^* = 0, 5, 10, 20$ (left-hand column) and $e^* = 0, 5, 10, 20$ (right-hand column) are depicted by continuous, dashed, dotted and dashed-dotted curves, respectively, in each panel. Panels (a) and (b) are for the case with no torsion ($\psi^* = 0$); panels (c) and (d) correspond to $\psi^* = 0.5$; for panels (e) and (f), $\psi^* = 1$.

6. Concluding remarks

In the foregoing sections the influence of the deformation dependence of the dielectric permittivity of an electroelastic tube subject to finite deformations consisting of axial extension, radial inflation and torsion has been highlighted, and it is clear that this dependence and the torsion have a significant effect compared with corresponding results for constant permittivity given in [1] in the absence of torsion. That the permittivity does indeed depend on deformation has been demonstrated in several papers, including [2] and [3]. The model of the deformation dependence adopted herein reflects the properties found in these papers for particular materials. However, information concerning the deformation dependent properties are rather limited and to inform a definitive model for these properties many more data are needed.

References

[1] A. Melnikov, R.W. Ogden, Finite deformations of an electroelastic circular cylindrical tube, Z. Angew. Math. Phys. 67 (2016) 140.

[2] G. Kofod, P. Sommer-Larsen, R. Kornbluh, R. Pelrine, Actuation response of polyacrylate dielectric elastomers, J. Intell. Mater. Syst. Struct. 14 (2003) 787–793.

[3] M. Wissler, E. Mazza, Electromechanical coupling in dielectric elastomer actuators, Sens. Actuators A 138 (2007) 384–393.

[4] X. Zhao, Z. Suo, Electrostriction in elastic dielectrics undergoing large deformation, J. Appl. Phys. 104 (2008) 123530.

[5] S.M.A. Jiménez, R.M. McMeeking, Deformation dependent dielectric permittivity and its effect on actuator performance and stability, Int. J. Non-Lin. Mech. 57 (2013) 183–191.

[6] M. Gei, S. Colonnelli, R. Springhetti, The role of electrostriction on the stability of dielectric elastomer actuators, Int. J. Solids Structures 51 (2014) 848–860.

[7] J. Zhu, H. Stoyanov, G. Kofod, Z. Suo, Large deformation and electromechanical instability of a dielectric elastomer tube actuator, J. Appl. Phys. 108 (2010) 074113.

[8] A.N. Gent, A new constitutive relation for rubber, Rubber Chem. Technol. 69 (1996) 59–61.

[9] G.A. Maugin, Continuum Mechanics of Electromagnetic Solids, North Holland, Amsterdam 1988.

[10] A.C. Eringen, G.A. Maugin, Electrodynamics of Continua, Springer, New York 1990.

[11] R.W. Ogden, Non-linear Elastic Deformations, Dover Publications, New York, 1997.

[12] L. Dorfmann, R.W. Ogden, Nonlinear Theory of Electroelastic and Magnetoelastic Interactions, Springer-Verlag, New York 2014.

[13] L. Dorfmann, R.W. Ogden, Nonlinear electroelasticity: material properties, continuum theory and applications, Proc. R. Soc. Lond. A 2017.0311.

[14] A. Dorfmann, R.W. Ogden, Nonlinear electroelasticity, Acta Mech. 174 (2005) 167–183.

[15] A. Dorfmann, R.W. Ogden, Nonlinear electroelastic deformations, J. Elast. 82 (2006) 99–127.

[16] L. Dorfmann, R.W. Ogden, Instabilities of an electroelastic plate, Int. J. Eng. Sci. 77 (2014) 79–101.

[17] R.S. Rivlin, Torsion of a rubber cylinder, J. Appl. Phys. 18 (1947) 444–449.

[18] R.S. Rivlin, Large elastic deformations of isotropic materials IV. Further developments of the general theory, Phil. Trans. R. Soc. Lond. A 241 (1948) 379–397.

[19] M. Singh, A.C. Pipkin, Controllable states of elastic dielectrics, Arch. Rat. Mech. Anal. 21 (1966) 169–210.

[20] Wolfram Research, Inc., Mathematica, Version 11, Champaign (2017).